Tetrahedron 65 (2009) 496–503

Contents lists available at ScienceDirect

Tetrahedron

journal homepage: www.elsevier.com/locate/tet

Synthesis, binding properties and theoretical studies of *p*-*tert*-butylhexahomotrioxacalix[3]arene tri(adamantyl)ketone with alkali, alkaline earth, transition, heavy metal and lanthanide cations

Paula M. Marcos [a,b,*], José R. Ascenso [c], Manuel A.P. Segurado [a,b], Raul J. Bernardino [d], Peter J. Cragg [e]

[a] Centro de Ciências Moleculares e Materiais, Faculdade de Ciências da Universidade de Lisboa, Edifício C8, 1749-016 Lisboa, Portugal
[b] Faculdade de Farmácia da Universidade de Lisboa, Av. Prof. Gama Pinto, 1649-003 Lisboa, Portugal
[c] Instituto Superior Técnico, Complexo I, Av. Rovisco Pais, 1049-001 Lisboa, Portugal
[d] Escola Superior de Tecnologia do Mar, Instituto Politécnico de Leiria, Santuário N.ª Sra. dos Remédios, Apartado 126, 2524-909 Peniche, Portugal
[e] School of Pharmacy and Biomolecular Sciences, University of Brighton, Brighton BN2 4GJ, UK

ARTICLE INFO

Article history:
Received 29 September 2008
Received in revised form 26 October 2008
Accepted 4 November 2008
Available online 8 November 2008

Keywords:
Calixarenes
Hexahomotrioxacalix[3]arene ketone
Metal cation extraction
Proton NMR titration
Molecular mechanics
Ab initio

ABSTRACT

p-*tert*-Butylhexahomotrioxacalix[3]arene tri(adamantyl)ketone (**1b**) was synthesized for the first time. Compound **1b** was obtained in a cone conformation in solution at room temperature, as established by NMR spectroscopy (^{1}H and ^{13}C). The binding properties of ligand **1b** for alkali, alkaline earth, transition, heavy metal and lanthanide cations have been assessed by phase transfer and proton NMR titration experiments. Molecular mechanics and ab initio techniques were also employed to complement the NMR data. The results are compared to those obtained with other closely related homooxacalixarene derivatives. Although triketone **1b** is a weak extractant, it shows a strong peak selectivity for Na^{+} and also some preference for Ag^{+}. Proton NMR titrations indicate the formation of 1:1 complexes between **1b** and the cations studied, and also that they should be located inside the cavity defined by the phenoxy and carbonyl oxygen atoms. Although the molecular mechanics results show little correlation with the NMR data, a good agreement was obtained with the ab initio models.

1. Introduction

The importance of calixarenes[1–3] in host–guest chemistry, even after more than three decades of research, is due to their relatively easy functionalization on both the upper and lower rims, giving a great variety of derivatives, which can become versatile molecular platforms for the design of supramolecular structures.

In particular, the ability of carbonyl containing substituents on the lower rim of calixarenes to bind metal ions, predominantly alkali and alkaline earth,[4,5] but also transition, heavy metal[6,7] and lanthanide[8,9] cations, has been largely studied. At the same time, homooxacalixarenes,[10,11] which derive from calixarenes by replacement of one or more CH_2 bridges by CH_2OCH_2 groups, have also been investigated. Among them, hexahomotrioxacalix[3]arenes have received significant attention as receptors, mainly due to their structural features:[12] a cavity formed by a 18-membered ring, only two basic conformations (cone and partial cone) and a C_3-symmetry. However, and despite these features, the studies of the ionophoric abilities of hexahomotrioxacalix[3]arenes bearing carbonyl groups at their lower rims towards metal cations are scarce compared to those of the calix[4]arene analogues. A few examples of derivatives containing ester,[13,14] carboxylic acid[15] and amide[16,17] groups are reported in the literature.

Following our previous studies on the synthesis and binding properties of homooxacalixarenes bearing carbonyl groups at the lower rim, namely amide[18,19] and ketone[20,21] functions, towards a large variety of cations, we obtained a new hexahomotrioxacalix[3]arene derivative. This paper reports the synthesis, the NMR conformational analysis and the binding properties of *p*-*tert*-butylhexahomotrioxacalix[3]arene tri(adamantyl)ketone (**1b**) towards alkali, alkaline earth, transition (Mn^{2+}, Fe^{2+}, Co^{2+}, Ni^{2+}, Cu^{2+} and Zn^{2+}), heavy metal (Ag^{+}, Cd^{2+} and Pb^{2+}) and lanthanide (La^{3+}, Ce^{3+}, Pr^{3+}, Nd^{3+}, Sm^{3+}, Eu^{3+}, Gd^{3+}, Dy^{3+}, Er^{3+} and Yb^{3+}) cations. These properties have been assessed by extraction studies with the corresponding metal picrates from an aqueous solution into dichloromethane and by proton NMR titrations. In the absence of X-ray structures, theoretical studies using molecular mechanics and ab initio techniques were employed to complement the information given by the NMR data. The results are compared to those obtained with other closely related homooxacalixarene

* Corresponding author. Centro de Ciências Moleculares e Materiais, Faculdade de Ciências da Universidade de Lisboa, Edifício C8, 1749-016 Lisboa, Portugal. Tel.: +351 21 7500111; fax: +351 21 7500979.
E-mail address: pmmarcos@fc.ul.pt (P.M. Marcos).

0040-4020/$ – see front matter © 2008 Elsevier Ltd. All rights reserved.
doi:10.1016/j.tet.2008.11.005

derivatives, and discussed in terms of substituents, size and conformational effects of the macrocycles.

To the best of our knowledge, this is the first report on the synthesis and ion binding properties of a hexahomotrioxacalix[3]arene ketone derivative.

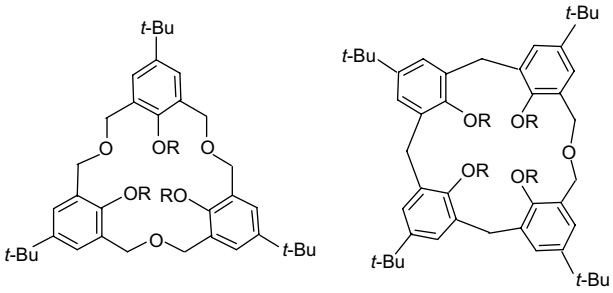

1a R = H
1b R = CH_2COAd
1c R = $CH_2CON(Et)_2$

2a R = H
2b R = CH_2COAd

2. Results and discussion

2.1. Synthesis and NMR conformational analysis

Treatment of compound **1a** with 1-adamantyl bromomethyl ketone and sodium hydride in dry THF under reflux furnished the hexahomotrioxacalix[3]arene triketone **1b**. Proton and carbon-13 NMR experiments were carried out in chloroform at room temperature to establish its conformation.

The C_3-symmetry in triketone **1b** is reflected by its proton and carbon NMR spectra. The ^1H NMR spectrum displays one AB quartet for the CH_2 bridge protons and one singlet for the *tert*-butyl and aromatic protons. In addition, the OCH_2COAd groups exhibit one singlet for the CH_2 protons and a series of multiplets for the Ad groups. The ^{13}C NMR spectrum shows a pattern containing five downfield resonances arising from the carbonyl and aromatic carbon atoms, two midfield resonances arising from the methylene carbon atoms of the OCH_2COAd and CH_2OCH_2 groups, and six upfield resonances arising from the quaternary carbon atoms of the Ad and *tert*-butyl groups (2 lines), the secondary and tertiary carbon atoms of the Ad group (3 lines) and the methyl carbon atoms of the *tert*-butyl group (1 line). All resonances were assigned by DEPT experiments.

As was mentioned before, this kind of calixarene can exist in only two basic conformations (cone and partial cone). Thus, those spectra clearly indicate the cone conformation for compound **1b**.

2.2. Extraction studies

The ionophoric properties of triketone **1b** towards alkali, alkaline earth, transition, heavy metal and lanthanide cations were evaluated by the standard picrate extraction method.[22] The results, expressed as a percentage of cation extracted (%*E*), are reported in Tables 1 and 2. The corresponding values for compounds **1c**[19] and **2b**[20,21] are included for comparison.

The results obtained with ketone **1b** range from 4 to 20% for the alkali cations and from 2 to 4% for the alkaline earth cations (Table 1). These data reveal that **1b** is a weak extractant for both groups of cations, except for Na^+ (20%), for which it shows a significant preference. In fact, ketone **1b**, although displaying much lower extraction percentages than triamide **1c**, exhibits a sharper peak selectivity for Na^+ than **1c** ($S_{Na^+/K^+}=3.9$ and 1.6 for **1b** and **1c**, respectively). However, within these series of cations, both hexahomotrioxacalix[3]arene derivatives show similar extraction profiles. Compared to its dihomooxacalix[4]arene tetraketone analogue **2b**, compound **1b** is a much weaker extractant for all the cations. This is due presumably to its higher conformational flexibility. The replacement of the methylene bridges by dimethyleneoxa bridges in triketone **1b** increases its flexibility. The $\Delta G^{\neq}$ barriers for conformational inversion in $CDCl_3$ are <9 and 12.9 kcal mol^{-1} for the parent calixarenes **1a** and **2a**, respectively.[23] Furthermore, **1b** possesses only three ketone groups and consequently only six donating sites can surround the cations, compared to the eight sites of the tetraketone.

In the case of the transition and heavy metal cations (Table 1) a similar situation can be observed. Compound **1b** is also a poor extractant showing, however, some preference for Ag^+ (13%). An extraction profile favouring Ag^+ over Pb^{2+} is now observed for **1b** ($S_{Ag^+/Pb^{2+}}=2.6$), an inverse trend to that shown by triamide **1c** ($S_{Pb^{2+}/Ag^+}=2$). The ketone behaviour is similar to those already found for other dihomooxa ketone derivatives.[21] Although these ligands contain hard oxygen donor atoms, they display a clear preference for Ag^+, a soft Lewis acid.

The extraction of lanthanide cations by both adamantyl ketones was studied in this work (Table 2). Triketone **1b** is practically unable to discriminate among the ten lanthanides investigated and is a weak phase transfer agent (%*E* ranges from 5 to 7). The lack of donating groups may be even more relevant here, as lanthanides require high coordination numbers (8 or 9).[24] Tetraketone **2b** shows higher percentages (%*E* ranges from 6 to 23) and preference for the heavy lanthanides Gd^{3+} and Yb^{3+} (23 and 21%, respectively). The extraction trend observed for both ketones is similar, but this behaviour is the opposite of that found by us for the corresponding amide derivatives.[25]

2.3. Proton NMR studies

To obtain further information on the cation binding behaviour of triketone **1b**, specifically concerning the binding sites, proton NMR titrations in $CDCl_3$ were performed. The cations studied were Na^+, K^+, Ca^{2+}, Sr^{2+}, Ba^{2+}, Zn^{2+}, Ag^+, Pb^{2+}, La^{3+}, Eu^{3+} and Yb^{3+}. Different situations were found after the addition of the salts to the ligand. No complexation was observed in the cases of Zn^{2+}, Eu^{3+} and Yb^{3+} and in all other cases the experimental data were consistent with the formation of 1:1 complexes only.

Table 1
Percentage extraction of alkali, alkaline earth, transition and heavy metal picrates into CH_2Cl_2 at 25 °C[a]

	Li^+	Na^+	K^+	Rb^+	Cs^+	Mg^{2+}	Ca^{2+}	Sr^{2+}	Ba^{2+}	Mn^{2+}	Fe^{2+}	Co^{2+}	Ni^{2+}	Cu^{2+}	Zn^{2+}	Ag^+	Cd^{2+}	Pb^{2+}
Ionic radius[b]/Å	0.78	0.98	1.33	1.49	1.65	0.78	1.06	1.27	1.43	0.83	0.78	0.75	0.69	0.73	0.75	1.15	0.95	1.18
1b	4.0	20	5.2	5.6	5.5	2.0	4.1	3.9	3.9	2.4	5.2	1.5	3.6	4.3	3.3	13	3.0	5.0
2b[c]	23	82	85	66	30	13	15	23	63	7.0	11	5.2	7.0	31	21	80	15	43
1c[d]	25	50	32	27	20	17	34	41	55	19	19	39	45	24	15	40	37	80

[a] Values with uncertainties less than 5%.
[b] Goldschmidt, V. M. *Skrifter Norske Videnskaps-Akad. Oslo, I*, Mat.-Naturv. Kl, **1926** and Shannon, R. D.; Prewitt, C. T. *Acta Crystallogr.* **1969**, *B25*, 925; **1970**, *B26*, 1046; data quoted in Marcus, I. *Ion Properties*; Marcel Dekker: New York, NY, 1997; pp 46–47.
[c] Data taken from Refs. 20 and 21.
[d] Data taken from Ref. 19.

Table 2
Percentage extraction of lanthanide picrates into CH_2Cl_2 at 25 °C[a]

	La^{3+}	Ce^{3+}	Pr^{3+}	Nd^{3+}	Sm^{3+}	Eu^{3+}	Gd^{3+}	Dy^{3+}	Er^{3+}	Yb^{3+}
Ionic radius[b]/Å	1.03	1.01	0.99	0.98	0.96	0.95	0.94	0.91	0.89	0.87
1b	6.0	5.1	4.5	5.6	5.9	5.7	5.9	5.3	6.0	6.8
2b	9.3	7.7	6.0	8.4	14	7.4	23	7.9	12	21

[a] Values with uncertainties less than 5%.
[b] Shannon, R. D.; Prewitt, C. T. *Acta Crystallogr.* **1969**, *B25*, 925; **1970**, *B26*, 1046; data quoted in Marcus, I. *Ion Properties*; Marcel Dekker: New York, NY, 1997; pp 46–47.

Variable amounts of the salts were added to ketone **1b** and the proton spectra were recorded after each addition. These titrations indicate similar behaviours for Na^+ and the divalent cations. With [salt]/[ligand] ratios lower than one, sharp signals of the complexed and uncomplexed ligand are present in the spectra (for Ca^{2+} and Sr^{2+} they are slightly broad), indicating that on the NMR time scale the exchange rate between the two species is slow, at room temperature. This behaviour reflects a high affinity of ligand **1b** for these cations. Upon reaching 1:1 ratios, all the signals for the free ligand disappear and those of the complexed ligand remain unaltered after subsequent addition of the salts, indicating a 1:1 metal-to-ligand stoichiometry. In contrast, titrations of **1b** with K^+ and Ag^+ initially induce broadening of the signals until the [salt]/[ligand] ratio reaches the unity, when the signals become sharp. This indicates a fast exchange rate between the two species on the NMR time scale, at room temperature. Again, the NMR titrations suggest a 1:1 stoichiometry, since no further spectral changes are observed after subsequent additions of the salts.

Proton NMR data of the free and complexed ligand **1b** are collected in Table 3. Complexation of the cations affects all the proton chemical shifts in the ligand, except in the cases of Zn^{2+}, Eu^{3+} and Yb^{3+} where there are no variations, as already mentioned. The largest variations are recorded for the aromatic protons and the methylene protons of the OCH_2CO groups, which move downfield, and by the oxygen bridge equatorial methylene protons (CH_2OCH_2), which move upfield. The smallest variations are observed for the protons of the adamantyl and *tert*-butyl groups. Identical situation was already found for triamide **1c**.[19]

It has been observed that the chemical shift changes of the methylene protons of the OCH_2CO groups in dihomooxacalix[4]-arene amide[18] and ketone[20,21] derivatives are upfield for the monovalent cations and downfield for the divalent ones. A close examination of the spectral changes upon complexation indicates that triketone **1b** behaves in a slightly different way. Except for Ba^{2+}, which shows a small upfield shift, all the cations experience downfield shift changes. However, the divalent cations still show much higher variations than the monovalent and also the trivalent cations. The highest value was recorded for Pb^{2+} ($\Delta\delta$=0.68 ppm) and the lowest for La^{3+} ($\Delta\delta$=0.05 ppm). This behaviour of ketone **1b** is closer to that of the hexahomotrioxacalix[3]arene amide derivative (**1c**), studied previously.[19]

Table 3
Proton chemical shifts (δ, ppm) of ligand **1b** and its 1:1 metal complexes in $CDCl_3$

	t-Bu	Ad	CH_2OCH_2			OCH_2CO	ArH
			eq	ax	$\Delta\delta$		
1b	1.09	1.67–2.02	4.49	4.75	0.26	4.85	6.91
1b+Na^+	1.23	1.70–2.12	4.19	4.50	0.31	5.03	7.25
1b+K^+	1.20	1.70–2.08	4.23	4.84	0.61	4.95	7.13
1b+Ca^{2+}	1.22	1.73–2.12	4.33	4.82	0.49	5.27	7.23
1b+Sr^{2+}	1.19	1.72–2.10	4.29	4.86	0.57	5.09	7.19
1b+Ba^{2+}	1.13	1.68–2.05	4.31	4.70	0.39	4.78	6.99
1b+Zn^{2+}	1.10	1.67–2.03	4.48	4.76	0.28	4.86	6.91
1b+Ag^+	1.24	1.70–2.11	4.24	4.69	0.45	5.02	7.28
1b+Pb^{2+}	1.21	1.75–2.14	4.31	4.83	0.52	5.53	7.21
1b+La^{3+}	1.13	1.68–2.04	4.38	4.86	0.48	4.90	6.95
1b+Eu^{3+}	1.10	1.67–2.03	4.48	4.75	0.27	4.87	6.91
1b+Yb^{3+}	1.10	1.67–2.03	4.49	4.76	0.27	4.87	6.91

For other calixarenes, the variation in chemical shifts experienced by the equatorial methylene protons of the $ArCH_2Ar$ bridges is downfield and much smaller than that of the axial protons, but the $ArCH_2OCH_2Ar$ bridges behave differently, as reported before.[13,18–21] The equatorial methylene protons of the oxygen bridges move upfield and experience larger shift variations than the axial ones. These results suggest that the oxygen bridge conformation changes significantly upon complexation, with the equatorial protons undergoing a higher shielding effect. The maximum value was recorded for Na^+ ($\Delta\delta$=0.30 ppm) and the minimum for La^{3+} ($\Delta\delta$=0.11 ppm). All the monovalent cations show higher shift changes than the divalent ones. Gutsche[26] established that the difference in the chemical shifts between the axial and equatorial protons of the $ArCH_2Ar$ bridges indicates the degree of flattening of the cone conformation. A value around 0.9 ppm means a regular cone conformation and zero a regular 1,3-alternate conformation. Upon complexation with all eight cations the $\Delta\delta_{Hax-Heq}$ increases (Table 3). If Gutsche's criterion is also applicable to the CH_2OCH_2 bridges, it indicates that the phenyl groups in triketone **1b** are more flattened than those in calix[4]arenes and dihomooxacalix[4]arenes, and stand up when the cations enter into the ionophoric cavity, resulting in a more regular cone conformation upon complexation. Interestingly, the highest difference is observed for K^+ ($\Delta\delta$=0.61 ppm) and the lowest for Na^+ ($\Delta\delta$=0.31 ppm).

The deshielding effect observed for the aromatic protons indicates the involvement of the phenolic oxygens in complexation, as reported previously.[27] The largest shift changes shown by the protons adjacent to the oxygen donor atoms can be explained in terms of variations of both shielding and deshielding effects of the aromatic rings and carbonyl groups upon cation binding to those donor atoms. Therefore, this suggests that the cations must be inside the cavity defined by the phenoxy and carbonyl oxygen atoms and bound through metal–oxygen interactions.

The magnitude of the chemical shift variations for triketone **1b** follows the order: $Na^+ > Ag^+ \approx Ca^{2+} \approx Pb^{2+} > Sr^{2+} \approx K^+ > Ba^{2+} > La^{3+}$. From this trend, Na^+ is the best bound cation, followed by comparable spectral changes among Ag^+, Ca^{2+} and Pb^{2+}. These results reflect the extraction data, particularly the preference for the monovalent cations Na^+ and Ag^+. Although lanthanides are hard Lewis acids and have strong affinity towards hard oxygen donor atoms, they are the poorest bound cations. This may be due to the fact that lanthanide cations require high coordination numbers (8 or 9) and therefore the six donating sites available in triketone **1b** are not enough to promote a strong complexation. That magnitude order for **1b** suggests that, more important than the charge (mono, di or trivalent) and nature (hard, soft or intermediate) of the cations, the size is the main factor affecting complexation. An average cation size of 1.09 Å seems to best match the cavity dimensions of **1b**. It is worthwhile to point out that among the three lanthanides studied, only La^{3+} (ionic radius of 1.03 Å) was complexed.

2.4. Theoretical studies

Energy minimized structures were calculated using molecular mechanics for **1b** and its metal cation complexes to mirror those used in the NMR experiments. In previous work this method has met with some success,[19] however, here analysis of the molecular mechanics results revealed little correlation with the NMR data. Table 4 gives data related to the coordination environment around the cations studied. Na^+, K^+, Ca^{2+} and Zn^{2+} were predicted to be bound within the cavity defined by the lower rim and bridging oxygen atoms. For these cations the geometry of **1b** was quite

Table 4
Summary of molecular modelling experiments

Complex	Position of cation[a]	M^{n+}–O interactions[b]		Aromatic centroid separation
1b·Na^+	−1.92	Carbonyl	2.35	5.5
		Alkyl ether	2.37[c]	
		Aryl ether	2.49[c]	
1b·K^+	−2.07	Alkyl ether	2.69[c]	5.6
		Aryl ether	2.74[c]	
		Carbonyl	2.75	
1b·Ca^{2+}	−1.61	Carbonyl	2.36	5.4
		Alkyl ether	2.55[c]	
		Aryl ether	2.65	
1b·Sr^{2+}	5.44[d]			5.4
1b·Ba^{2+}	3.45[d]			5.4
1b·Zn^{2+}	−1.61	Carbonyl	2.11	5.4
		Aryl ether	2.66	
1b·Ag^+	−3.78	Alkyl ether	4.20[c]	5.4
1b·Pb^{2+}	8.13[d]			5.2
1b·La^{3+}	9.70[d]			5.2

All distances in Å.
[a] Relative to the plane defined by the three alkyl ether oxygen atoms in **1b**.
[b] Less than 5 Å; mean distance of three closest contacts unless otherwise stated.
[c] Single interaction.
[d] Outside macrocyclic cavity.

regular with the three aromatic rings adopting pseudo-C_{3v} symmetry. Ag^+ interacts weakly with the lower rim of **1b** and the remaining cations, Sr^{2+}, Ba^{2+}, Pb^{2+} and La^{3+}, do not appear to interact at all. In these five examples the macrocycle has a highly distorted upper rim geometry. Examples of these binding motifs are illustrated in Figure 1. It has been noted that gas phase models of solution behaviour often break down at low levels of theory[28] so a more sophisticated ab initio approach was adopted.

Although the comparison between gas phase and condensed phase structures is not direct, as evidenced by the molecular mechanics results, all the structures were optimized solvent free in the ab initio simulations. They are therefore expected to correlate primarily with gas state complex geometries and not necessarily with the extractability from aqueous solution data, in which the solvent will influence the metal–ligand interactions and relative complexation energies.

Four different binding modes were obtained for the metal complexes studied. They are illustrated in Figure 2, together with the predicted structure of ligand **1b** (Fig. 2a). The structural data for **1b** complexes are reported in Table 5. The binding mode for Na^+, K^+ and Ag^+ complexes (Fig. 2b) shows the cations slightly below the plane defined by the three phenoxy oxygen atoms, interacting mainly with the three carbonyl oxygen atoms and also with two of the phenoxy oxygen atoms ('3+2' interaction), as shown by the distances given in Table 5. In the case of Zn^{2+}, Sr^{2+} and Ba^{2+} complexes (Fig. 2c) a '3+2' interaction mode is also observed, but with the adamantyl groups more distant from each other. For Ca^{2+} and La^{3+} complexes (Fig. 2d), the cations coordinate with the six oxygen atoms in a higher position within **1b**, especially for Ca^{2+}. For all these complexes, the presence of the cation imposes slightly shorter distances among the *tert*-butyl groups and slightly larger distances among the adamantyl groups, comparing to free ligand **1b**. The results of the ab initio optimized structures towards Ca^{2+} and La^{3+} are consistent with the NMR data. Both cations induce approximately the same chemical shift variations for the aromatic and methylenic protons of the OCH_2CO groups as, for example, for Ca^{2+} ($\Delta\delta$=0.32 and 0.42 ppm, respectively). For the remaining cations a slight discrepancy between the NMR and the ab initio data was found, mainly in the case of Na^+, K^+ and Ag^+ (see Table 3). For these cations the aromatic protons undergo a larger chemical shift variation than the OCH_2CO methylenic protons, suggesting a stronger interaction with the phenoxy oxygen atoms than with the carbonyl oxygen atoms. Finally for Pb^{2+} complex (Fig. 2e) the cation is in the lowest position within **1b**, in the same plane as the adamantyl groups, interacting with the three carbonyl oxygen atoms only, and presenting the highest dipole moment. This is in agreement with the NMR data, as Pb^{2+} induces the largest chemical shift variation for the methylene protons of the OCH_2CO groups ($\Delta\delta$=0.68 ppm) and a much smaller one ($\Delta\delta$=0.30 ppm) for the aromatic protons. This difference suggests that Pb^{2+} cation strongly interacts with the carbonyl oxygens than with the phenoxy oxygens. Moreover, it also induces the largest chemical shifts for the adamantyl protons, among all the cations.

The ab initio calculations also predict that the oxygen atoms of the $ArCH_2OCH_2Ar$ bridges do not participate in metal binding, since average distances from the cations to the mean plane of the three bridge oxygen atoms are too great for such an interaction (Table 5). A similar situation was already mentioned for a closely related hexahomotrioxacalix[3]arene derivative.[13]

In order to determine the electrostatic equilibriums in the different complexes, maps of electrostatic potential were calculated over an electronic isodensity surface of ρ=0.04 $Å^{-3}$ (Fig. 3). On these surfaces, the red regions are those of relatively lower or more negative electrostatic potential and the blue regions correspond to

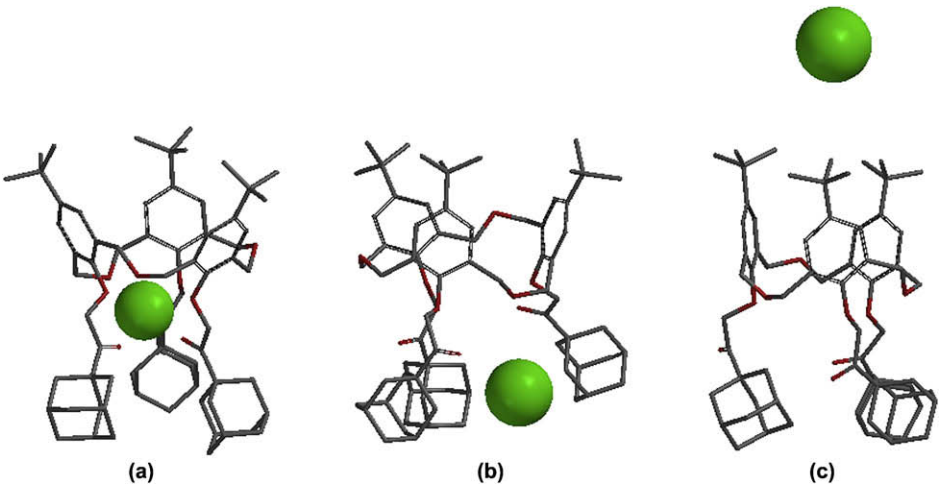

Figure 1. Optimized molecular mechanics structures for **1b**–metal complexes (a) Na^+, K^+, Ca^{2+} and Zn^{2+}, (b) Ag^+ and (c) Sr^{2+}, Ba^{2+}, Pb^{2+} and La^{3+}. All the hydrogens were removed for clarity.

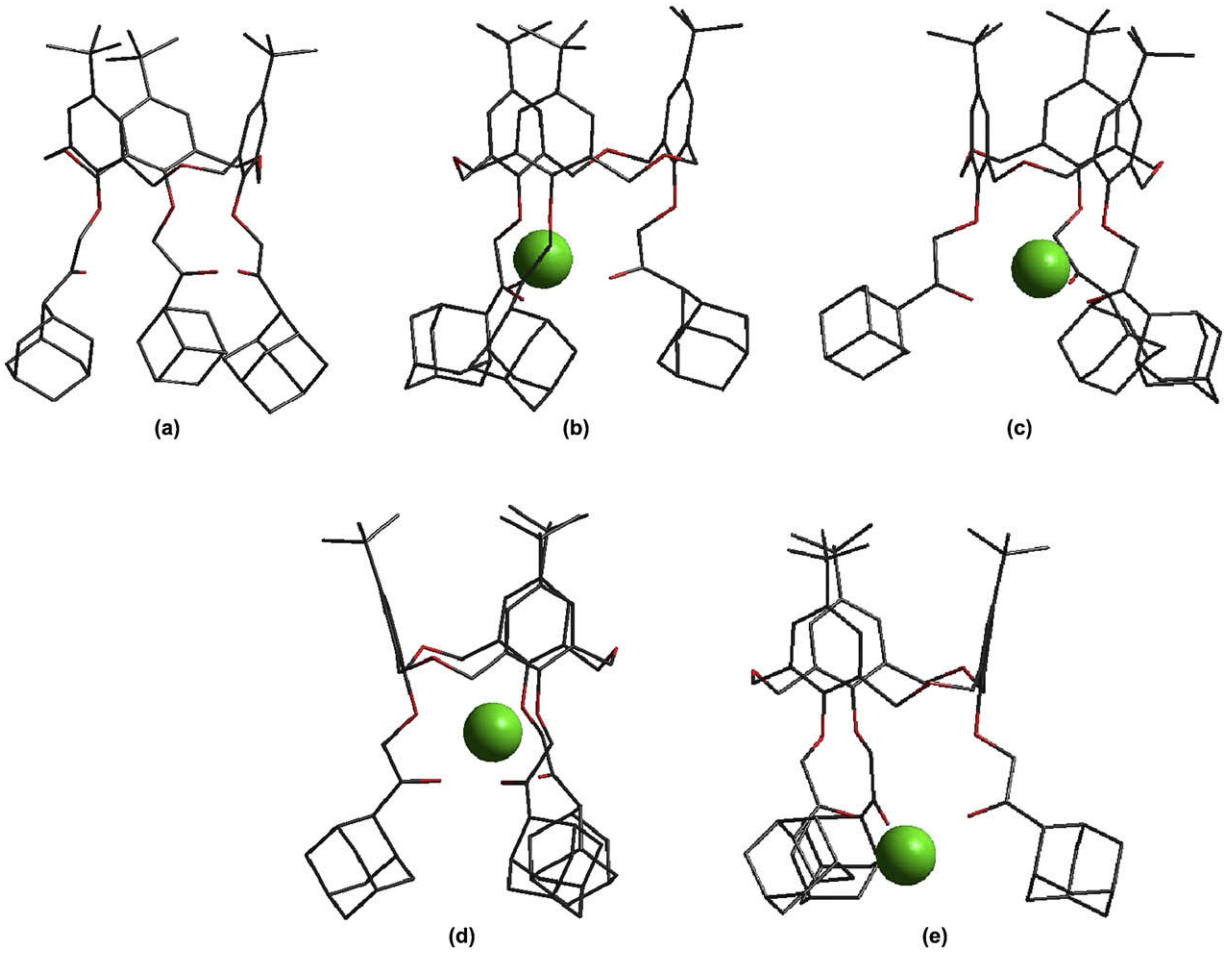

Figure 2. Optimized ab initio structures for **1b**–metal complexes (a) **1b**, (b) Na^+, K^+ and Ag^+, (c) Zn^{2+}, Sr^{2+} and Ba^{2+}, (d) Ca^{2+} and La^{3+} and (e) Pb^{2+}. All the hydrogens were removed for clarity.

higher or more positive electrostatic potential, as seen in the associated scale. Each cation produces a visible reorganization of all the charges in the ligand as shown, for example, in the case of Zn^{2+} (Fig. 3c). Although this structure is very similar to that of **1b** (Fig. 3a), the presence of high positive potential zones can make this complex less likely to be stabilized by the solvent. Contrarily, the Na^+ complex (Fig. 3b) shows a charge distribution closer to that of ligand **1b**, which may indicate a better solvent stabilization for this complex. These interpretations are in agreement with the NMR data, where Na^+ is the best bound cation.

From the complexation energies reported in Table 6, the following order was observed: $La^{3+}>Zn^{2+}>Ca^{2+}>Sr^{2+}>Pb^{2+}>Ba^{2+}>Na^+>Ag^+>K^+$. As with the molecular mechanics results, this order of stability does not exactly match the NMR sequence as the two most stable complexes observed in the ab initio model (La^{3+} and Zn^{2+}) are among the least stable complexes in the NMR. This

Table 5
Structural data of **1b** complexes (HF/6-31G)

	Position cation[a] (Å)	O_{carb}–metal[b] (Å)	$O_{phen.}$–metal[b] (Å)	(C–C)$_{tert}$[c] (Å)	Dipole moment (Debye)	Metal charge[d]	O_{carb} charge[d]	O_{phen} charge[d]
1b	—	—	—	6.37, 7.13, 7.43	7.30	—	−0.561	−0.784
1b·Na^+	−3.37	2.28	2.42, 2.45, 4.80	6.23	4.26	+0.722	−0.628	−0.850, −0.839, −0.795
1b·K^+	−3.77	2.65	2.85, 2.96, 5.14	6.14	4.28	+0.789	−0.626	−0.813, −0.818, −0.793
1b·Ca^{2+}	−1.64	2.45	2.49	8.35, 6.54, 6.92	4.95	+1.694	−0.696	−0.912
1b·Sr^{2+}	−3.54	2.44	2.59, 2.62, 5.15	6.14	7.63	+1.500	−0.710, −0.707, −0.769	−0.791, −0.904, −0.905
1b·Ba^{2+}	−3.75	2.62	2.80, 2.84, 5.30	5.80	7.90	+1.528	−0.755, −0.705, −0.702	−0.883, −0.882, −0.789
1b·Zn^{2+}	−3.24	2.02	2.12, 2.22, 4.80	6.77, 5.95, 6.18	7.26	+1.460	−0.699, −0.805, −0.726	−0.788, −0.922, −0.956
1b·Ag^+	−3.61	2.43	2.70, 2.71, 4.91	6.17	3.98	+0.586	−0.611	−0.817
1b·Pb^{2+}	−5.58	2.31	4.43, 4.57, 5.56	6.24	17.32	+1.556	−0.781, −0.785, −0.846	−0.796
1b·La^{3+}	−2.61	2.44	2.54	6.44	4.51	+2.239	−0.747	−0.993

[a] Distance between the cation position and the plane defined by the three bridge oxygen atoms.
[b] Distance between the cation and each one of the oxygen atoms of the three carbonyl groups (O_{carb}) or the three phenoxy groups (O_{phen}). When values are similar the mean is presented.
[c] Distance between two adjacent tertiary carbons from the *tert*-butyl groups.
[d] Mulliken charges.

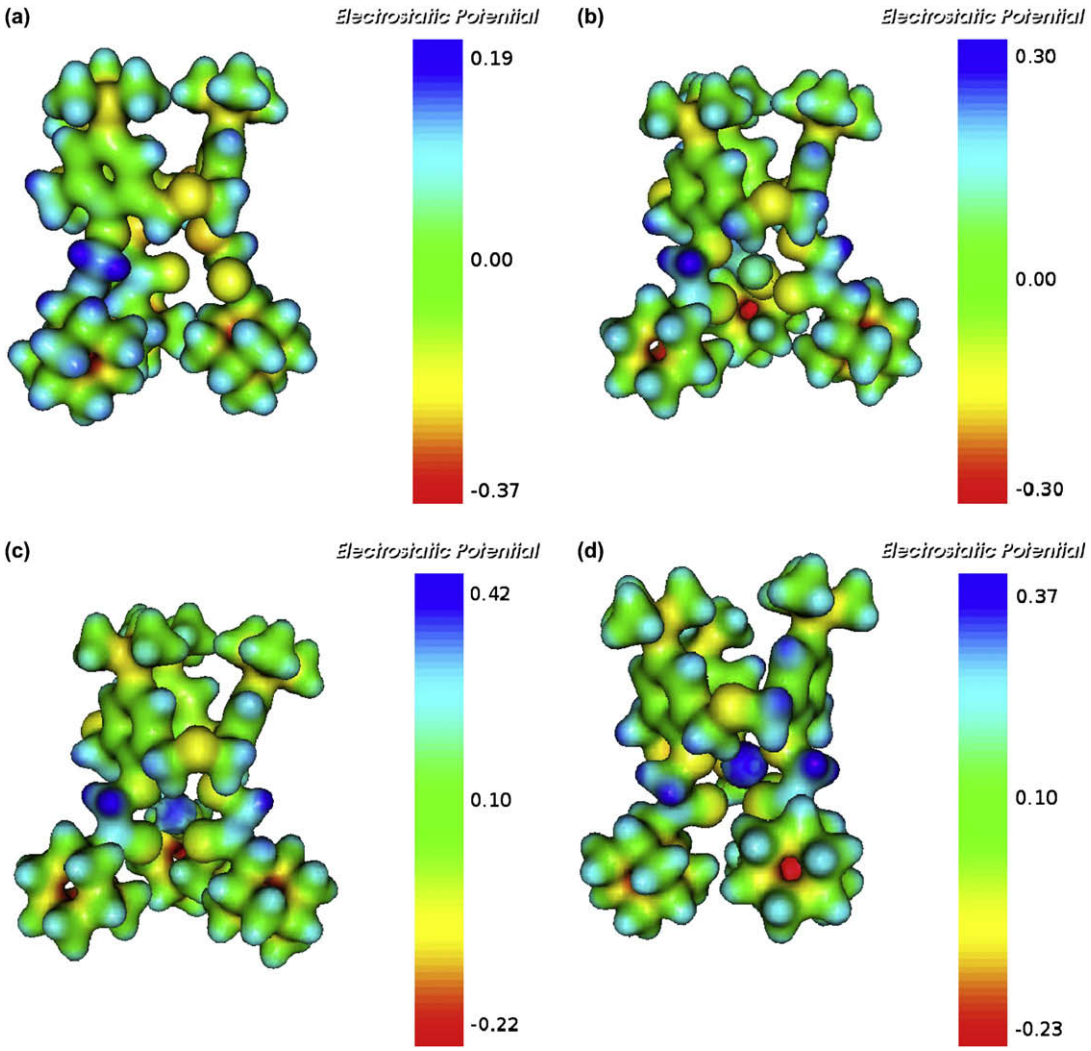

Figure 3. Electrostatic potential for **1b**–metal complexes. The electrostatic potential (in a.u.) is represented over a constant electronic isodensity ρ (in Å^{-3}) surfaces of volume V_s (in Å^{-3}). All figures correspond to ρ=0.05 Å^{-3}. (a) **1b**, (b) Na^+, (c) Zn^{2+} and (d) Ca^{2+}.

discrepancy is almost certainly related to the energy of metal desolvation and number of solvent molecules found in the metal's primary coordination sphere in the complex. In order to determine the importance of this process, the desolvation energies (Table 7) were calculated for each cation with six methanol molecules, except for Ag^+ and La^{3+}, where the coordination numbers are 2 and 9, respectively.[29] The larger desolvation energies associated with the more positive cations can make the complexation process considerably harder, and therefore be responsible for the behaviour observed, especially in the case of Zn^{2+}. For this cation, the desolvation barrier is almost two times the barriers associated with the other divalent cations, which may explain the lack of interaction between Zn^{2+} and **1b** observed in the NMR data.

Table 6
Total energies E (a.u.) and complexation energies ΔE_c (kcal mol^{-1})[a] for the systems studied

	HF/3-21G[b]		HF/6-31G[b]	
	E	ΔE_c	E	ΔE_c
1b	−3437.10452	—	−3454.74367	—
1b·Na^+	−3597.97122	−121.08	−3616.55910	−97.99
1b·K^+	−4033.26479	−96.44	−4053.82257	−67.28
1b·Ca^{2+}	−4110.42396	−323.63	−4131.33155	−303.71
1b·Sr^{2+}	−6554.00591	−222.25	−3484.90005[c]	−235.82
1b·Ba^{2+}	−3462.02825[c]	−221.66	−3479.63556[c]	−201.68
1b·Zn^{2+}	−5206.03696	−412.53	−5231.93634	−364.33
1b·Ag^+	−8610.88236	−111.25	−3600.73660[c]	−90.66
1b·Pb^{2+}	−3440.05393[c]	−226.76	−3457.67496[c]	−215.38
1b·La^{3+}	−3870.94318[c]	−557.16	−3888.51075[c]	−512.24

[a] ΔE_c corresponds to the process **1b**+M^{n+}→[**1b**−M^{n+}], where M^{n+} represents each one of the cations.
[b] Optimized geometries at this level of theory.
[c] Energies obtained with the referred level of theory for all atoms except the cation. For the cations the Stuttgart/Dresden ECP basis set was used.

3. Conclusions

Hexahomotrioxacalix[3]arene triketone **1b** was synthesized and obtained in a cone conformation in solution at room temperature. Extraction studies with metal picrates from an aqueous solution into CH_2Cl_2 have shown that ketone **1b** is a weak extracting agent. However, **1b** exhibits a sharp peak selectivity for Na^+ and also some preference for Ag^+. The low extraction percentages obtained with **1b** are, presumably, due to its higher conformational flexibility compared to its dihomooxacalix[4]arene tetraketone analogue **2b**. Moreover, **1b** possesses only three ketone groups and consequently only six donating sites can surround the cations. The NMR data support the extraction results, particularly the preference for the monovalent cations Na^+ and Ag^+. Ligand **1b** forms 1:1 complexes

Table 7
Desolvation energies ΔE_d (kcal mol^{-1})[a] for the systems studied

		Na^+	K^+	Ca^{2+}	Sr^{2+}	Ba^{2+}	Zn^{2+}	Ag^+	Pb^{2+}	La^{3+}
HF/6-31G[b]	ΔE_d[a]	+87.49	+54.16	+241.95	+222.14[c]	+188.42[c]	+352.55	+61.42[c]	+205.83[c]	+640.00[c]

[a] ΔE_d corresponds to the process $[M(MeOH)_6]^{n+} \rightarrow M^{n+} + 6MeOH$, where M represents each one of the cations; for Ag^+ and La^{3+} the coordination numbers are 2 and 9, respectively.
[b] Optimized geometries at this level of theory.
[c] Energies obtained with the referred level of theory for all atoms except the cation. For the cations the Stuttgart/Dresden ECP basis set was used.

with Na^+, K^+, Ca^{2+}, Sr^{2+}, Ba^{2+}, Ag^+, Pb^{2+} and La^{3+}, and no complexation with Zn^{2+}, Eu^{3+} and Yb^{3+}. The structures of these complexes deduced from NMR experiments show that the cations should be encapsulated in the cavity composed of the phenoxy and carbonyl oxygen atoms. A certain discrepancy was observed between the molecular mechanics results and the NMR data. Nevertheless, at a higher level of theory, the ab initio model predicted positions for the bound cations that agree with the NMR data, although it does not satisfactorily explain the strength of the metal binding.

4. Experimental

4.1. Synthesis

All chemicals were reagent grade and were used without further purification. Melting points were measured on a Stuart Scientific apparatus and are uncorrected. ^1H and ^{13}C NMR spectra were recorded on a Bruker Avance III 500 MHz spectrometer, with TMS as internal reference. Elemental analysis was determined on a Fisons EA 1108 microanalyser.

*4.1.1. 7,15,23-Tri-tert-butyl-25,26,27-triadamantylketone-2,3,10,11,18,19-hexahomo-3,11,19-trioxacalix[3]arene (**1b**)*

To a stirred solution of 2.0 g (3.47 mmol) of *p-tert*-butylhexahomotrioxacalix[3]arene (**1a**) in 100 mL of dry THF was added 0.63 g (21 mmol) of sodium hydride (80% oil dispersion) followed by 4.12 g (16 mmol) of 1-adamantyl bromomethyl ketone. The reaction mixture was refluxed under N_2 for 24 h. The solvent was then evaporated, and a yellow oily residue was obtained and poured into a volume of 160 mL of H_2O/CH_2Cl_2. This mixture was stirred for about 1 h and, after separating the phases, the organic layer was washed several times with 1 M HCl solution and water, and dried with anhydrous Na_2SO_4. Evaporation of the solvent gave a yellow oily residue, to which cold ethanol was added. A white solid was obtained by filtration and then recrystallization from dichloromethane/ethanol afforded the pure compound **1b** (0.84 g, 22 %) as white crystals: mp 205–207 °C. ^1H NMR ($CDCl_3$, 500 MHz) δ 1.09 (s, 27H, $C(CH_3)_3$), 1.67–2.02 (m, 45H, Ad), 4.49, 4.75 (ABq, 12H, J=13.3 Hz, CH_2OCH_2), 4.85 (s, 6H, OCH_2CO), 6.91 (s, 6H, ArH); ^{13}C NMR ($CDCl_3$, 125.8 MHz) δ 27.9 (CH, Ad), 31.5 ($C(CH_3)_3$), 34.2 ($C(CH_3)_3$), 36.6, 38.0 (CH_2, Ad), 45.1 (C, Ad), 69.4 (CH_2OCH_2), 75.1 (OCH_2CO), 126.0 (ArH), 131.1, 145.9, 154.0 (Ar), 210.0 (CO). Anal. Calcd for $C_{72}H_{96}O_9$: C, 78.22; H, 8.75. Found: C, 77.85; H, 8.98.

4.2. Extraction studies

Equal volumes (5 mL) of aqueous solutions of metal picrates (2.5×10^{-4} M) and solutions of the calixarenes (2.5×10^{-4} M) in CH_2Cl_2 were vigorously shaken for 2 min, and then thermostated in a water bath with mechanical stirring at 25 °C overnight. After complete phase separation, the concentration of picrate ion in the aqueous phase was determined spectrophotometrically (λ_{max}=354 nm). For each cation–calixarene system the absorbance measurements were repeated, at least, four times. Blank experiments showed negligible picrate extraction in the absence of a calixarene. The details of the transition metal picrate preparation have already been described.[30] All the other metal picrates (alkali, alkaline earth, heavy and lanthanides) were also prepared using the same method. Thus, they were prepared by adding an excess of the respective metal carbonate in a hot (80–90 °C) and saturated aqueous picric acid solution. After filtration of the unreacted carbonate, the solution was concentrated and cooled until precipitation was complete. The crystals of metal picrates were then recrystallized from hot aqueous solutions. For the Ag(I) picrate preparation, silver oxide was used instead of silver carbonate. Due to the light sensitivity of the silver salts, the procedure was done avoiding direct light.

4.3. Proton NMR titration experiments

Several aliquots (up to 2–3 equiv) of the salt solutions (0.25 M) in CD_3OD were added to $CDCl_3$ solutions (0.5×10^{-2} M) of ligand **1b** directly in the NMR tube. The salts used were Na and K thiocyanates, Ca, Sr and Pb perchlorates, and Ba, Ag, Zn, La, Eu and Yb triflates. Due to the low solubility of Eu triflate in MeOH, it was necessary to decrease the concentration of the ligand (0.25×10^{-3} M) and of the salt (4.17×10^{-3} M). The spectra were recorded on a Bruker Avance III 500 Spectrometer after each addition of the salts. The temperature of the NMR probe was kept constant at 22 °C.

4.4. Experimental theoretical methods

4.4.1. Molecular modelling studies

The coordinates of the ligand and a cation held within the cavity defined by the amide groups were taken from an X-ray structure in which adamantyl groups were substituted for amides.[31] The initial structure for each complex was generated by systematically changing the cation. An unconstrained geometry optimisation was then carried out on each structure using the Merck Molecular Force Field (MMFF94) within the Spartan '06 software suite.[32]

4.4.2. Ab initio studies

The structures of ketone **1b** and its cation complexes were fully optimized without symmetry constraints using the Hartree–Fock (HF) method, which is well known to produce accurate geometries. An initial guess for all the structures was made using the small basis set 3-21G before reoptimized using the larger 6-31G basis set. For the larger cations, the binding energies were calculated by using effective core potentials (ECP) on the metal, derived from energy adjusted ab initio pseudopotential methods in the Gaussian 03 software package.[33] The vibrational frequency calculations were performed at the same level of theory to check that all structures were global minima of the potential energy surface (denoted by an absence of negative vibrational frequencies) and to correct the computed energies for zero-point energies as well as translational, rotational, and vibrational contributions to the enthalpy. All calculations were performed with the Gaussian 03 and all the figures and electrostatic potential surfaces were constructed using the Molekel software.[34]

This study started with a search for minimum energy conformations using several initial geometries, taking in account that

each of the cations could electrostatically interact with: (a) one or more of the three aromatic rings; (b) one or more oxygens from the oxygen bridges; (c) with one or more oxygens of the phenoxy and carbonyl groups. After optimizing these initial possibilities, the global minimum configurations were used for the final optimization study with the larger basis set.

The electrostatic potential for the **1b**–metal complexes were drawn over a surface of constant electronic isodensity using Molekel software. All the data needed to generate these surfaces and electrostatic potentials were calculated with Gaussian 03 software.

The relative complexation energies (ΔE_c corresponding to the process $\mathbf{1b}+M^{n+}\rightarrow[\mathbf{1b}-M^{n+}]$, where M^{n+} represents each one of the cations) were calculated as the energy difference at 298 K between the final energy of the complexes and the sum of the energies of **1b** and the cation in study, at the same theoretical level.[35]

References and notes

1. Gutsche, C. D. In *Calixarenes Revisited*; Stoddart, J. F., Ed.; The Royal Society of Chemistry: Cambridge, 1998.
2. *Calixarenes in Action*; Mandolini, L., Ungaro, R., Eds.; Imperial College Press: London, 2000.
3. *Calixarenes 2001*; Asfari, Z., Böhmer, V., Harrofield, J., Vicens, J., Eds.; Kluwer Academic: Dordrecht, 2001.
4. McKervey, M. A.; Schwing-Weill, M. J.; Arnaud-Neu, F. In *Comprehensive Supramolecular Chemistry*; Lehn, J. M., Gokel, G. W., Eds.; Elsevier: Oxford, 1996; Vol. 1, pp 537–603.
5. Arnaud-Neu, F.; McKervey, M. A.; Schwing-Weill, M. J. In *Calixarenes 2001*; Asfari, Z., Böhmer, V., Harrowfield, J., Vicens, J., Eds.; Kluwer Academic: Dordrecht, 2001; pp 385–406.
6. Ludwig, R. *Fresenius' J. Anal. Chem.* **2000**, *367*, 103.
7. Roundhill, D. M.; Shen, J. Y. In *Calixarenes 2001*; Asfari, Z., Böhmer, V., Harrowfield, J., Vicens, J., Eds.; Kluwer Academic: Dordrecht, 2001; pp 407–420.
8. Arnaud-Neu, F. *Chem. Soc. Rev.* **1994**, 235.
9. Arnaud-Neu, F. *Radiochim. Acta* **2003**, *91*, 659.
10. Masci, B. In *Calixarenes 2001*; Asfari, Z., Böhmer, V., Harrowfield, J., Vicens, J., Eds.; Kluwer Academic: Dordrecht, 2001; pp 235–249.
11. (a) Shokova, E. A.; Kovalev, V. V. *Russ. J. Org. Chem.* **2004**, *40*, 607; (b) Shokova, E. A.; Kovalev, V. V. *Russ. J. Org. Chem.* **2004**, *40*, 1547.
12. Araki, K.; Inada, K.; Otsuka, H.; Shinkai, S. *Tetrahedron* **1993**, *49*, 9465.
13. Araki, K.; Hashimoto, N.; Otsuka, H.; Shinkai, S. *J. Org. Chem.* **1993**, *58*, 5958.
14. Yamato, T.; Zhang, F.; Tsuzuki, H.; Miura, Y. *Eur. J. Org. Chem.* **2001**, 1069.
15. Arnaud-Neu, F.; Cremin, S.; Harris, S.; McKervey, M. A.; Schwing-Weill, M. J.; Schwinté, P.; Walker, A. *J. Chem. Soc., Dalton Trans.* **1997**, 329.
16. Matsumoto, T.; Nishio, S.; Takeshita, M.; Shinkai, S. *Tetrahedron* **1995**, *51*, 4647.
17. Yamato, T.; Zhang, F. *J. Inclusion Phenom. Macrocyclic Chem.* **2001**, *39*, 55.
18. Marcos, P. M.; Félix, S.; Ascenso, J. R.; Segurado, M. A. P.; Pereira, J. L. C.; Khazaeli-Parsa, P.; Hubscher-Bruder, V.; Arnaud-Neu, F. *New J. Chem.* **2004**, *28*, 748.
19. Marcos, P. M.; Ascenso, J. R.; Cragg, P. J. *Supramol. Chem.* **2007**, *19*, 199.
20. Marcos, P. M.; Félix, S.; Ascenso, J. R.; Segurado, M. A. P.; Mellah, B.; Abidi, R.; Hubscher-Bruder, V.; Arnaud-Neu, F. *Supramol. Chem.* **2006**, *18*, 285.
21. Marcos, P. M.; Félix, S.; Ascenso, J. R.; Segurado, M. A. P.; Thuéry, P.; Mellah, B.; Michel, S.; Hubscher-Bruder, V.; Arnaud-Neu, F. *New J. Chem.* **2007**, *31*, 2111.
22. Pedersen, C. *J. Am. Chem. Soc.* **1970**, *92*, 391.
23. Gutsche, C. D.; Bauer, L. J. *J. Am. Chem. Soc.* **1985**, *107*, 6052.
24. Cotton, S. A. *C. R. Chim.* **2005**, *8*, 129.
25. Marcos, P. M.; Ascenso, J. R.; Segurado, M. A. P.; Cragg, P. J.; Hubscher-Bruder, V.; Arnaud-Neu, F. manuscript in preparation.
26. Gutsche, C. D. In *Calixarenes*; Stoddart, J. F., Ed.; The Royal Society of Chemistry: Cambridge, 1989.
27. Arduini, A.; Pochini, A.; Reverberi, S.; Ungaro, R.; Andreetti, G.; Ugozzoli, F. *Tetrahedron* **1986**, *42*, 2089.
28. Sheehan, R.; Cragg, P. J. *Supramol. Chem.* **2008**, *20*, 443.
29. Lee, J. D. *Concise Inorganic Chemistry*; Wiley-Blackwell: Oxford, 1999.
30. Marcos, P. M.; Ascenso, J. R.; Segurado, M. A. P.; Pereira, J. L. C. *J. Inclusion Phenom. Macrocyclic Chem.* **2002**, *42*, 281.
31. Cragg, P. J.; Allen, M. C.; Steed, J. W. *Chem. Commun.* **1999**, 553.
32. Spartan '06, Wavefunction Inc., Irvin, CA 92612, USA.
33. Frisch, M. J.; Trucks, G. W.; Schlegel, H. B.; Scuseria, G. E.; Robb, M. A.; Cheeseman, J. R.; Montgomery, J. A., Jr.; Vreven, T.; Kudin, K. N.; Burant, J. C.; Millam, J. M.; Iyengar, S. S.; Tomasi, J.; Barone, V.; Mennucci, B.; Cossi, M.; Scalmani, G.; Rega, N.; Petersson, G. A.; Nakatsuji, H.; Hada, M.; Ehara, M.; Toyota, K.; Fukuda, R.; Hasegawa, J.; Ishida, M.; Nakajima, T.; Honda, Y.; Kitao, O.; Nakai, H.; Klene, M.; Li, X.; Knox, J. E.; Hratchian, H. P.; Cross, J. B.; Adamo, C.; Jaramillo, J.; Gomperts, R.; Stratmann, R. E.; Yazyev, O.; Austin, A. J.; Cammi, R.; Pomelli, C.; Ochterski, J. W.; Ayala, P. Y.; Morokuma, K.; Voth, G. A.; Salvador, P.; Dannenberg, J. J.; Zakrzewski, V. G.; Dapprich, S.; Daniels, A. D.; Strain, M. C.; Farkas, O.; Malick, D. K.; Rabuck, A. D.; Raghavachari, K.; Foresman, J. B.; Ortiz, J. V.; Cui, Q.; Baboul, A. G.; Clifford, S.; Cioslowski, J.; Stefanov, B. B.; Liu, G.; Liashenko, A.; Piskorz, P.; Komaromi, I.; Martin, R. L.; Fox, D. J.; Keith, T.; Al-Laham, M. A.; Peng, C. Y.; Nanayakkara, A.; Challacombe, M.; Gill, P. M. W.; Johnson, B.; Chen, W.; Wong, M. W.; Gonzalez, C.; Pople, J. A. *Gaussian 03, Revision B.03*; Gaussian: Pittsburgh, PA, 2003.
34. Flükiger, P.F. Molekel, Molecular Visualisation Software; University of Geneva (http://www.bioinformatics.org/molekel/wiki/).
35. Bernardino, R. J.; Cabral, B. J. C. *Supramol. Chem.* **2002**, *14*, 57.